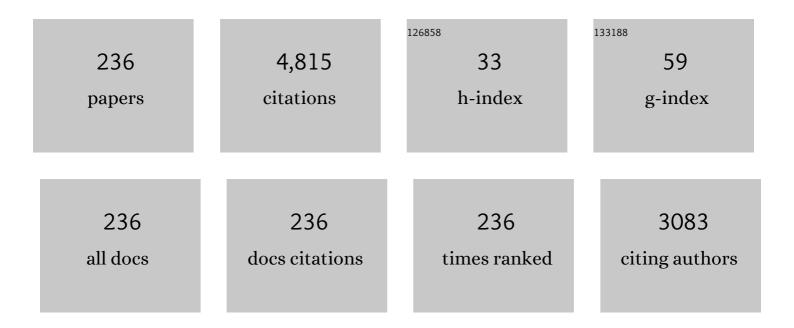
## Mitsuru Takenaka

List of Publications by Year in descending order

Source: https://exaly.com/author-pdf/7110101/publications.pdf Version: 2024-02-01



#	Article	IF	CITATIONS
1	Effective Mobility Enhancement Through Asymmetric Strain Channels on Extremely Thin Body (100) GOI pMOSFETs. IEEE Transactions on Electron Devices, 2022, 69, 25-30.	1.6	6
2	A floating gate negative capacitance MoS <sub>2</sub> phototransistor with high photosensitivity. Nanoscale, 2022, 14, 2013-2022.	2.8	11
3	Optimum Channel Design of Extremely-Thin-Body nMOSFETs Utilizing Anisotropic Valley—Robust to Surface Roughness Scattering. IEEE Transactions on Electron Devices, 2022, 69, 2115-2121.	1.6	5
4	Introduction of high tensile strain into Ge-on-Insulator structures by oxidation and annealing at high temperature. Japanese Journal of Applied Physics, 2022, 61, SC1027.	0.8	0
5	Verification of influence of tail states and interface states on sub-threshold swing of Si n-channel MOSFETs over a temperature range of 4–300 K. Japanese Journal of Applied Physics, 2022, 61, SC1032.	0.8	11
6	Numerical analysis of optical phase modulator operating at 2 μm wavelength using graphene/III–V hybrid metal-oxide-semiconductor capacitor. Japanese Journal of Applied Physics, 2022, 61, SC1031.	0.8	1
7	Modulation bandwidth improvement of III-V/Si hybrid MOS optical modulator by reducing parasitic capacitance. Optics Express, 2022, 30, 22848.	1.7	4
8	Monolithic integration of electro-absorption modulators and photodetectors on III-V CMOS photonics platform by quantum well intermixing. Optics Express, 2022, 30, 23318.	1.7	3
9	Electrical Properties of Ultra-Thin Body (111) Ge-On-Insulator n-Channel MOSFETs Fabricated by Smart-Cut Process. IEEE Journal of the Electron Devices Society, 2021, 9, 612-617.	1.2	3
10	Impacts of Equivalent Oxide Thickness Scaling of TiN/Yâ,,Oâ,ƒ Gate Stacks With Trimethylaluminum Treatment on SiGe MOS Interface Properties. IEEE Electron Device Letters, 2021, 42, 966-969.	2.2	5
11	Si racetrack optical modulator based on the Ill–V/Si hybrid MOS capacitor. Optics Express, 2021, 29, 6824.	1.7	12
12	Silicon Photonics Using Heterogeneous Integration for Society 5.0. Vacuum and Surface Science, 2021, 64, 68-73.	0.0	0
13	Advanced CMOS technologies for ultra-low power logic and AI applications. , 2021, , .		2
14	Proposal and Experimental Demonstration of Ultrathin-Body (111) InAs-On-Insulator nMOSFETs With L Valley Conduction. IEEE Transactions on Electron Devices, 2021, 68, 2003-2009.	1.6	7
15	7â€5: <i>Invited Paper:</i> Bilayer Tunneling Field Effect Transistors using Oxide Semiconductor/Groupâ€IV Semiconductor Heteroâ€structures. Digest of Technical Papers SID International Symposium, 2021, 52, 73-76.	0.1	0
16	Si microring resonator optical switch based on optical phase shifter with ultrathin-InP/Si hybrid metal-oxide-semiconductor capacitor. Optics Express, 2021, 29, 18502.	1.7	5
17	Antiferroelectric properties of ZrO2 ultra-thin films prepared by atomic layer deposition. Applied Physics Letters, 2021, 118, .	1.5	10
18	Re-examination of effects of ALD high-k materials on defect reduction in SiGe metal–oxide–semiconductor interfaces. AIP Advances, 2021, 11, .	0.6	2

#	Article	IF	CITATIONS
19	Evaluation of interface traps inside the conduction band of InAs-on-insulator nMOSFET by self-consistent Hall-QSCV method. Applied Physics Letters, 2021, 119, .	1.5	2
20	Germanium Mid-infrared Integrated Photonics on GeOI Platform. , 2021, , .		0
21	Thermo-optic Mach–Zehnder Interferometer Integrated with Si PN Diode Switch for Bipolar Optical Phase Control. , 2021, , .		0
22	Monolithic Integration of III-V/Si Hybrid MOS Optical Phase Shifter and InGaAs Membrane Photodetector. , 2021, , .		1
23	Ge Ring Modulator Based on Carrier-injection Phaser Shifter Operating at Two Micrometer Band. , 2021, , .		1
24	Low-loss Ge waveguide at the 2-µm band on an n-type Ge-on-insulator wafer. Optical Materials Express, 2021, 11, 4097.	1.6	9
25	Optimum Design of Channel Material and Surface Orientation for Extremely-Thin-Body nMOSFETs under New Modeling of Surface Roughness Scattering. , 2021, , .		3
26	Tunable Germanium-on-Insulator Band-Stop Optical Filter Using Thermo-Optic Effect. IEEE Photonics Journal, 2020, 12, 1-7.	1.0	4
27	Influence of layer transfer and thermal annealing on the properties of InAs-On-Insulator films. Journal of Applied Physics, 2020, 128, .	1.1	4
28	Impact of Switching Voltage on Complementary Steep-Slope Tunnel Field Effect Transistor Circuits. IEEE Transactions on Electron Devices, 2020, 67, 3876-3882.	1.6	1
29	Corrections to "Operation of (111) Ge-on-Insulator n-channel MOSFET Fabricated by Smart-Cut Technology―[Jul 20 985-988]. IEEE Electron Device Letters, 2020, 41, 1266-1266.	2.2	1
30	Reduction of MOS Interface Defects in TiN/Yâ,,Oâ,ƒ/Siâ,€.â,‡â,^Geâ,€.â,,â,, Structures by Trimethylaluminum Trea Transactions on Electron Devices, 2020, 67, 4067-4072.	tment. IEE I.6	E 17
31	Improved Ferroelectric/Semiconductor Interface Properties in Hf <sub>0.5</sub> Zr <sub>0.5</sub> O <sub>2</sub> Ferroelectric FETs by Low-Temperature Annealing. IEEE Electron Device Letters, 2020, 41, 1588-1591.	2.2	65
32	High responsivity in MoS2 phototransistors based on charge trapping HfO2 dielectrics. Communications Materials, 2020, 1, .	2.9	51
33	Metal–oxide–semiconductor interface properties of TiN/Y2O3/Si0.62Ge0.38 gate stacks with high temperature post-metallization annealing. Journal of Applied Physics, 2020, 127, .	1.1	10
34	Efficient Mid-Infrared Germanium Variable Optical Attenuator Fabricated by Spin-on-Glass Doping. Journal of Lightwave Technology, 2020, 38, 4808-4816.	2.7	6
35	Operation of (111) Ge-on-Insulator n-Channel MOSFET Fabricated by Smart-Cut Technology. IEEE Electron Device Letters, 2020, 41, 985-988.	2.2	13
36	Evaluation of polarization characteristics in metal/ferroelectric/semiconductor capacitors and ferroelectric field-effect transistors. Applied Physics Letters, 2020, 116, .	1.5	44

#	Article	IF	CITATIONS
37	p-Channel TFET Operation of Bilayer Structures With Type-II Heterotunneling Junction of Oxide- and Group-IV Semiconductors. IEEE Transactions on Electron Devices, 2020, 67, 1880-1886.	1.6	15
38	Improvement in Electrical Characteristics of ZnSnO/Si Bilayer TFET by W/Alâ,,Oâ, $f$ Gate Stack. IEEE Journal of the Electron Devices Society, 2020, 8, 341-345.	1.2	4
39	Computational design of efficient grating couplers using artificial intelligence. Japanese Journal of Applied Physics, 2020, 59, SGGE09.	0.8	11
40	Requirements of epitaxially grown InGaAs channel layers for tunnel field-effect transistors. Journal of Applied Physics, 2020, 127, 225702.	1.1	1
41	Diffusion properties of n-type dopants diffused from spin on glass into Ge. Journal of Applied Physics, 2020, 128, 015707.	1.1	Ο
42	Optical Phase Modulators Based on Reverse-Biased III-V/Si Hybrid Metal-Oxide-Semiconductor Capacitors. IEEE Photonics Technology Letters, 2020, 32, 345-348.	1.3	13
43	Si microring resonator crossbar arrays for deep learning accelerator. Japanese Journal of Applied Physics, 2020, 59, SGGE04.	0.8	18
44	Effects of hydrogen ion implantation dose on physical and electrical properties of Ge-on-insulator layers fabricated by the smart-cut process. AIP Advances, 2020, 10, .	0.6	7
45	Numerical analyses of optical loss and modulation bandwidth of an InP organic hybrid optical modulator. Optics Express, 2020, 28, 29730.	1.7	11
46	Taperless Si hybrid optical phase shifter based on a metal-oxide-semiconductor capacitor using an ultrathin InP membrane. Optics Express, 2020, 28, 35663.	1.7	7
47	Accurate evaluation of specific contact resistivity between InAs/Ni–InAs alloy using a multi-sidewall transmission line method. Japanese Journal of Applied Physics, 2020, 59, SGGA08.	0.8	5
48	Source engineering for bilayer tunnel field-effect transistor with hetero tunnel junction: thickness and impurity concentration. Applied Physics Express, 2020, 13, 074004.	1.1	7
49	Subband Engineering by Combination of Channel Thickness Scaling and (111) Surface Orientation in InAs-On-Insulator nMOSFETs. , 2020, , .		3
50	Taper-less III-V/Si Hybrid MOS Optical Phase Shifter using Ultrathin InP Membrane. , 2020, , .		2
51	Monolithic Germanium PIN Waveguide Photodetector Operating at 2 $\hat{1}$ /4m Wavelengths. , 2020, , .		2
52	Advanced MOS Device Technology for Low Power Logic LSI. , 2019, , .		0
53	Material design of oxide-semiconductor/group-IV-semiconductor bilayer tunneling field effect transistors. , 2019, , .		1
54	Fabrication and Electrical Characteristics of ZnSnO/Si Bilayer Tunneling Filed-Effect Transistors. IEEE Journal of the Electron Devices Society, 2019, 7, 1201-1208.	1.2	7

#	Article	IF	CITATIONS
55	Improvement of SiGe MOS interface properties with a wide range of Ge contents by using TiN/Y <sub>2</sub> O <sub>3</sub> gate stacks with TMA nassivation. , 2019, , .		15
56	Improvement of material quality of (100) and (111) Ge-on-insulator substrates fabricated by smart-cut technology. , 2019, , .		1
57	Bilayer tunneling field effect transistor with oxide-semiconductor and group-IV semiconductor hetero junction: Simulation analysis of electrical characteristics. AIP Advances, 2019, 9, 055001.	0.6	14
58	Impact of metal gate electrodes on electrical properties of Y2O3/Si0.78Ge0.22 gate stacks. Microelectronic Engineering, 2019, 214, 87-92.	1.1	8
59	ZnO/Si and ZnO/Ge bilayer tunneling field effect transistors: Experimental characterization of electrical properties. Journal of Applied Physics, 2019, 125, .	1.1	12
60	InGaSb-on-insulator p-channel metal-oxide-semiconductor field-effect transistors on Si fabricated by direct wafer bonding. Journal of Applied Physics, 2019, 125, .	1.1	6
61	Effects of ZrO <sub>2</sub> /Al <sub>2</sub> O <sub>3</sub> Gate-Stack on the Performance of Planar-Type InGaAs TFET. IEEE Transactions on Electron Devices, 2019, 66, 1862-1867.	1.6	25
62	Slow Trap Properties and Generation in Al <sub>2</sub> O <sub>3</sub> /GeO <sub><i>x</i></sub> /Ge MOS Interfaces Formed by Plasma Oxidation Process. ACS Applied Electronic Materials, 2019, 1, 311-317.	2.0	22
63	Fabrication of thin body InAs-on-insulator structures by Smart Cut method with H <sup>+</sup> implantation at room temperature. Japanese Journal of Applied Physics, 2019, 58, SBBA03.	0.8	9
64	Thermal properties of Ill–V on a SiC platform for photonic integrated circuits. Japanese Journal of Applied Physics, 2019, 58, SBBE06.	0.8	5
65	Drive current enhancement of Si MOSFETs by using anti-ferroelectric gate insulators. Japanese Journal of Applied Physics, 2019, 58, SBBA15.	0.8	5
66	Impact of SiGe layer thickness in starting substrates on strained Ge-on-insulator pMOSFETs fabricated by Ge condensation method. Applied Physics Letters, 2019, 114, .	1.5	15
67	Direct Observation of Interface Charge Behaviors in FeFET by Quasi-Static Split C-V and Hall Techniques: Revealing FeFET Operation. , 2019, , .		64
68	Strain and surface orientation engineering in extremely-thin body Ge and SiGe-on-insulator MOSFETs fabricated by Ge condensation. , 2019, , .		6
69	Coupled-Resonator-Induced-Transparency on Germanium-on-Insulator Mid-Infrared Platform. , 2019, , .		Ο
70	Re-examination of effects of sulfur treatment on Al2O3/InGaAs metal-oxide-semiconductor interface properties. Journal of Applied Physics, 2019, 126, .	1.1	6
71	Reduction of Slow Trap Density in Al <sub>2</sub> O <sub>3</sub> /GeO <sub> <i>x</i> </sub> N <sub> <i>y</i> </sub> /n-Ge MOS Interfaces by PPN-PPO Process. IEEE Transactions on Electron Devices, 2019, 66, 5060-5064.	1.6	4
72	III–V/Si Hybrid MOS Optical Phase Shifter for Si Photonic Integrated Circuits. Journal of Lightwave Technology, 2019, 37, 1474-1483.	2.7	34

Mitsuru Takenaka

#	Article	IF	CITATIONS
73	High-efficiency Ge thermo-optic phase shifter on Ge-on-insulator platform. Optics Express, 2019, 27, 6451.	1.7	10
74	Mid-infrared tunable Vernier filter on a germanium-on-insulator photonic platform. Optics Letters, 2019, 44, 2779.	1.7	9
75	Group IV/oxide semiconductor bi-layer tunneling FET. , 2019, , .		Ο
76	Design and characterization of Ge passive waveguide components on Ge-on-insulator wafer for mid-infrared photonics. Japanese Journal of Applied Physics, 2018, 57, 042202.	0.8	11
77	Pretreatment Effects on High-k/In <sub>x</sub> Ga <sub>1–x</sub> As MOS Interface Properties and Their Physical Model. IEEE Journal of the Electron Devices Society, 2018, 6, 487-493.	1.2	7
78	TiN/Al2O3/ZnO gate stack engineering for top-gate thin film transistors by combination of post oxidation and annealing. Applied Physics Letters, 2018, 112, .	1.5	11
79	Low-loss graphene-based optical phase modulator operating at mid-infrared wavelength. Japanese Journal of Applied Physics, 2018, 57, 04FH06.	0.8	8
80	Impact of Atomic Layer Deposition High k Films on Slow Trap Density in Ge MOS Interfaces With GeO <sub>x</sub> Interfacial Layers Formed by Plasma Pre-Oxidation. IEEE Journal of the Electron Devices Society, 2018, 6, 950-955.	1.2	13
81	Ge p-channel tunneling FETs with steep phosphorus profile source junctions. Japanese Journal of Applied Physics, 2018, 57, 04FD10.	0.8	10
82	Ge-on-Insulator Platform for Mid-Infrared Integrated Photonics. , 2018, , .		0
83	Characterization and understanding of slow traps in GeOx-based n-Ge MOS interfaces. , 2018, , .		5
84	Si Hybrid MOS Optical Phase Shifter for Switching and Computing. , 2018, , .		0
85	Semiconductor-insulator-semiconductor (SIS) structures for high-performance optical modulation. , 2018, , .		0
86	Hole mobility enhancement in extremely-thin-body strained GOI and SGOI pMOSFETs by improved Ge condensation method. , 2018, , .		9
87	III-V/Si Hybrid MOS Optical Phase Modulator for Si Photonic Integrated Circuits. , 2018, , .		0
88	Low-Power Ge Thermo-Optic Phase Shifter on Ge-on-Insulator Platform. , 2018, , .		0
89	Investigation of Electrical Characteristics of Vertical Junction Si n-Type Tunnel FET. IEEE Transactions on Electron Devices, 2018, 65, 5511-5517.	1.6	8
90	High-Q germanium optical nanocavity. Photonics Research, 2018, 6, 925.	3.4	20

Mitsuru Takenaka

#	Article	IF	CITATIONS
91	Relationship between interface state generation and substrate hole current in InGaAs metal-oxide-semiconductor (MOS) interfaces. Journal of Applied Physics, 2018, 123, 234502.	1.1	0
92	Group IV mid-infrared photonics [Invited]. Optical Materials Express, 2018, 8, 2276.	1.6	34
93	Mid-infrared high-Q germanium microring resonator. Optics Letters, 2018, 43, 2885.	1.7	39
94	InGaAsP Mach–Zehnder interferometer optical modulator monolithically integrated with InGaAs driver MOSFET on a III-V CMOS photonics platform. Optics Express, 2018, 26, 4842.	1.7	13
95	Influence of impurity concentration in Ge sources on electrical properties of Ge/Si hetero-junction tunneling field-effect transistors. Applied Physics Letters, 2018, 113, 062103.	1.5	12
96	Tunable Grating Coupler by Thermal Actuation and Thermo-Optic Effect. IEEE Photonics Technology Letters, 2018, 30, 1503-1506.	1.3	12
97	Ge photodetector monolithically integrated with amorphous Si waveguide on wafer-bonded Ge-on-insulator substrate. Optics Express, 2018, 26, 30546.	1.7	19
98	Ultra-power-efficient 2 × 2 Si Mach-Zehnder interferometer optical switch based on III-V/Si hybrid MOS phase shifter. Optics Express, 2018, 26, 35003.	1.7	22
99	Heterogeneous CMOS Photonics Based on SiGe/Ge and Ill–V Semiconductors Integrated on Si Platform. IEEE Journal of Selected Topics in Quantum Electronics, 2017, 23, 64-76.	1.9	19
100	Reduction of slow trap density of Al2O3/GeOx/n-Ge MOS interfaces by inserting ultrathin Y2O3 interfacial layers. Microelectronic Engineering, 2017, 178, 132-136.	1.1	7
101	Modulation of sub-threshold properties of InGaAs MOSFETs by La2O3 gate dielectrics. AIP Advances, 2017, 7, 095215.	0.6	6
102	Design and properties of planar-type tunnel FETs using In0.53Ga0.47As/InxGa1-xAs/In0.53Ga0.47As quantum well. Journal of Applied Physics, 2017, 122, .	1.1	12
103	Benchmarking Si, SiGe, and III–V/Si Hybrid SIS Optical Modulators for Datacenter Applications. Journal of Lightwave Technology, 2017, 35, 4047-4055.	2.7	22
104	Effects of HfO <sub>2</sub> /Al <sub>2</sub> O <sub>3</sub> gate stacks on electrical performance of planar ln <i> <sub>x</sub> </i> Ga <sub>1â^'</sub> <i> <sub>x</sub> </i> As tunneling field-effect transistors. Applied Physics Express, 2017, 10, 084201.	1.1	13
105	Efficient low-loss InGaAsP/Si hybrid MOS optical modulator. Nature Photonics, 2017, 11, 486-490.	15.6	166
106	III–V-based low power CMOS devices on Si platform. , 2017, , .		2
107	High performance 4.5-nm-thick compressively-strained Ge-on-insulator pMOSFETs fabricated by Ge condensation with optimized temperature control. , 2017, , .		8
108	Effects of impurity and composition profiles on electrical characteristics of GaAsSb/InGaAs hetero-junction vertical tunnel field effect transistors. Journal of Applied Physics, 2017, 122, .	1.1	19

#	Article	IF	CITATIONS
109	III–V/Ge MOSFETs and TFETs for ultra-low power logic LSIs. , 2017, , .		2
110	Near-infrared and mid-infrared integrated photonics based on Ge-on-insulator platform. , 2017, , .		1
111	III-V/Ge-based tunneling MOSFET. , 2017, , .		0
112	Effects of ge-source impurity concentration on electrical characteristics of Ge/Si hetero-junction tunneling FETs. , 2017, , .		0
113	Ultra-low power MOSFET and tunneling FET technologies using III-V and Ge. , 2017, , .		Ο
114	Proposal and demonstration of oxide-semiconductor/(Si, SiGe, Ge) bilayer tunneling field effect transistor with type-II energy band alignment. , 2017, , .		10
115	Mid-infrared germanium photonic crystal cavity. Optics Letters, 2017, 42, 2882.	1.7	27
116	InP-based photonic integrated circuit platform on SiC wafer. Optics Express, 2017, 25, 29993.	1.7	13
117	Focusing subwavelength grating coupler for mid-infrared suspended membrane germanium waveguides. Optics Letters, 2017, 42, 2094.	1.7	76
118	Influence of interface traps inside the conduction band on the capacitance–voltage characteristics of InGaAs metal–oxide–semiconductor capacitors. Applied Physics Express, 2016, 9, 111202.	1.1	5
119	InGaAsP variable optical attenuator with lateral P-I-N junction formed by Ni-InGaAsP and Zn diffusion on III-V on insulator wafer. MRS Advances, 2016, 1, 3295-3300.	0.5	5
120	InAs/GaSb-on-insulator single channel complementary metal-oxide-semiconductor transistors on Si structure. Applied Physics Letters, 2016, 109, 213505.	1.5	7
121	Properties of slow traps of ALD Al2O3/GeOx/Ge nMOSFETs with plasma post oxidation. Applied Physics Letters, 2016, 109, .	1.5	16
122	Analysis of interface trap density of plasma post-nitrided Al2O3/SiGe MOS interface with high Ge content using high-temperature conductance method. Journal of Applied Physics, 2016, 120, 125707.	1.1	12
123	Impact of surface orientation on (100), (111)A, and (111)B InGaAs surfaces with In content of 0.53 and 0.70 and on their Al2O3/InGaAs metal-oxide-semiconductor interface properties. Applied Physics Letters, 2016, 109, 182111.	1.5	7
124	Impact of La <inf>2</inf> 0 <inf>3</inf> /InGaAs MOS interface on InGaAs MOSFET performance and its application to InGaAs negative capacitance FET. , 2016, , .		2
125	Tunneling MOSFET technologies using III-V/Ge materials. , 2016, , .		14
126	III-V/Ge MOS device technologies for low power integrated systems. Solid-State Electronics, 2016, 125, 82-102.	0.8	41

#	Article	IF	CITATIONS
127	Novel Ge waveguide platform on Ge-on-insulator wafer for mid-infrared photonic integrated circuits. Optics Express, 2016, 24, 11855.	1.7	78
128	Effects of additional oxidation after Ge condensation on electrical properties of germanium-on-insulator p-channel MOSFETs. Solid-State Electronics, 2016, 117, 77-87.	0.8	7
129	Impact of Postdeposition Annealing Ambient on the Mobility of Ge nMOSFETs With 1-nm EOT Al <sub>2</sub> O <sub>3</sub> /GeO <sub><i>x</i></sub> /Ge Gate-Stacks. IEEE Transactions on Electron Devices, 2016, 63, 558-564.	1.6	11
130	First demonstration of SiGe-based carrier-injection Mach-Zehnder modulator with enhanced plasma dispersion effect. Optics Express, 2016, 24, 1979.	1.7	14
131	Characterization of ultrathin-body Germanium-on-insulator (GeOI) structures and MOSFETs on flipped Smart-Cutâ,,¢ GeOI substrates. Solid-State Electronics, 2016, 115, 120-125.	0.8	15
132	Low-dark-current waveguide InGaAs metal–semiconductor–metal photodetector monolithically integrated with InP grating coupler on III–V CMOS photonics platform. Japanese Journal of Applied Physics, 2016, 55, 04EH01.	0.8	11
133	Impact of thermal annealing on Ge-on-Insulator substrate fabricated by wafer bonding. Materials Science in Semiconductor Processing, 2016, 42, 259-263.	1.9	44
134	Experimental study on carrier transport properties in extremely-thin body Ge-on-insulator (GOI) p-MOSFETs with GOI thickness down to 2 nm. , 2015, , .		26
135	High <i>Ion</i> / <i>Ioff</i> and low subthreshold slope planar-type InGaAs tunnel field effect transistors with Zn-diffused source junctions. Journal of Applied Physics, 2015, 118, .	1.1	44
136	Surface Leakage Reduction in MSM InGaAs Photodetector on Ill–V CMOS Photonics Platform. IEEE Photonics Technology Letters, 2015, 27, 1569-1572.	1.3	16
137	Effectiveness of Surface Potential Fluctuation for Representing Inversion-Layer Mobility Limited by Coulomb Scattering in MOFETs. IEEE Electron Device Letters, 2015, 36, 1183-1185.	2.2	0
138	IIIâ $\in$ "V/Ge MOSFETs and tunneling FETs on Si platform for low power logic applications. , 2015, , .		4
139	Advanced nano CMOS using Ge/III–V semiconductors for low power logic LSIs. , 2015, , .		1
140	Numerical Analysis of Carrier-Depletion Strained SiGe Optical Modulators With Vertical p-n Junction. IEEE Journal of Quantum Electronics, 2015, 51, 1-7.	1.0	15
141	Suppression of dark current in GeO_x-passivated germanium metal-semiconductor-metal photodetector by plasma post-oxidation. Optics Express, 2015, 23, 16967.	1.7	28
142	Fabrication and MOS interface properties of ALD AlYO3/GeO /Ge gate stacks with plasma post oxidation. Microelectronic Engineering, 2015, 147, 244-248.	1.1	18
143	Ge/Si Heterojunction Tunnel Field-Effect Transistors and Their Post Metallization Annealing Effect. IEEE Transactions on Electron Devices, 2015, 62, 9-15.	1.6	37
144	Simulation of carrier-depletion strained SiGe optical modulators with vertical p-n junction. , 2014, , .		0

#	Article	IF	CITATIONS
145	Impact of Channel Orientation on Electrical Properties of Ge p- and n-MOSFETs With 1-nm EOT Al <sub>2</sub> O <sub>3</sub> /GeO <sub>x</sub> /Ge Gate-Stacks Fabricated by Plasma Postoxidation. IEEE Transactions on Electron Devices, 2014, 61, 3668-3675.	1.6	24
146	Impact of Plasma Postoxidation Temperature on the Electrical Properties of \${m Al}_{2}{m O}_{3}/{m GeO}_{x}/{m Ge}\$ pMOSFETs and nMOSFETs. IEEE Transactions on Electron Devices, 2014, 61, 416-422.	1.6	34
147	Low temperature Al_2O_3 surface passivation for carrier-injection SiGe optical modulator. Optics Express, 2014, 22, 7458.	1.7	8
148	Self-aligned Ni-GaSb source/drain junctions for GaSb p-channel metal-oxide-semiconductor field-effect transistors. Applied Physics Letters, 2014, 104, 093509.	1.5	22
149	Sb-Doped S/D Ultrathin Body Ge-On Insulator nMOSFET Fabricated by Improved Ge Condensation Process. IEEE Transactions on Electron Devices, 2014, 61, 3379-3385.	1.6	18
150	Physical understanding of electron mobility in asymmetrically strained InGaAs-on-insulator metal-oxide-semiconductor field-effect transistors fabricated by lateral strain relaxation. Applied Physics Letters, 2014, 104, 113509.	1.5	4
151	Strain-Modulated L-Valley Ballistic-Transport in (111) GaAs Ultrathin-Body nMOSFETs. IEEE Transactions on Electron Devices, 2014, 61, 1335-1340.	1.6	6
152	High Performance Tri-Gate Extremely Thin-Body InAs-On-Insulator MOSFETs With High Short Channel Effect Immunity and <inline-formula> <tex-math notation="TeX">\$V_{m th}\$ </tex-math></inline-formula> Tunability. IEEE Transactions on Electron Devices, 2014, 61, 1354-1360.	1.6	57
153	Waveguide InGaAs photodetector with schottky barrier enhancement layer on III-V CMOS photonics platform. , 2014, , .		0
154	Multi-bandgap III-V on insulator wafer fabricated by quantum well intermixing for III-V CMOS photonics platform. , 2014, , .		1
155	Surface orientation depdendence of electro-optic effects in InGaAsP for lateral PIN-junction InGaAsP photonic-wire modulators. , 2014, , .		0
156	InGaAs MSM photodetector monolithically integrated with InP photonic-wire waveguide on III-V CMOS photonics platform. IEICE Electronics Express, 2014, 11, 20140609-20140609.	0.3	15
157	Strain-induced enhancement of plasma dispersion effect and free-carrier absorption in SiGe optical modulators. Scientific Reports, 2014, 4, 4683.	1.6	45
158	Analysis and Comparison of L-Valley Transport in GaAs, GaSb, and Ge Ultrathin-Body Ballistic nMOSFETs. IEEE Transactions on Electron Devices, 2013, 60, 4213-4218.	1.6	19
159	High-Mobility Ge p- and n-MOSFETs With 0.7-nm EOT Using \$hbox{HfO}_{2}/hbox{Al}_{2}hbox{O}_{3}/hbox{GeO}_{x}/hbox{Ge}\$ Gate Stacks Fabricated by Plasma Postoxidation. IEEE Transactions on Electron Devices, 2013, 60, 927-934.	1.6	193
160	Impact of plasma post-nitridation on HfO2/Al2O3/SiGe gate stacks toward EOT scaling. Microelectronic Engineering, 2013, 109, 266-269.	1.1	19
161	High-Performance InAs-On-Insulator n-MOSFETs With Ni-InGaAs S/D Realized by Contact Resistance Reduction Technology. IEEE Transactions on Electron Devices, 2013, 60, 3342-3350.	1.6	38

MOS interface engineering for high-mobility Ge CMOS., 2013,,.

#	Article	IF	CITATIONS
163	High performance sub-20-nm-channel-length extremely-thin body InAs-on-insulator tri-gate MOSFETs with high short channel effect immunity and V <inf>th</inf> tunability. , 2013, , .		16
164	Experimental Study on Electron Mobility in In <sub>x</sub> Ga <sub>1-x</sub> As-on-Insulator Metal-Oxide-Semiconductor Field-Effect Transistors With In Content Modulation and MOS Interface Buffer Engineering. IEEE Nanotechnology Magazine, 2013, 12, 621-628.	1.1	28
165	Sub-60-nm Extremely Thin Body \${m ln}_{x}{m Ga}_{1-x}{m As}\$-On-Insulator MOSFETs on Si With Ni-InGaAs Metal S/D and MOS Interface Buffer Engineering and Its Scalability. IEEE Transactions on Electron Devices, 2013, 60, 2512-2517.	1.6	40
166	Evaluation of chemical potential for graphene optical modulators based on the semiconductor-metal transition. , 2013, , .		3
167	Low temperature surface passivation for carrier injection type SiGe optical modulator. , 2013, , .		0
168	Impact of Al <inf>2</inf> O <inf>3</inf> ALD temperature on Al <inf>2</inf> O <inf>3</inf> /GaSb metal-oxide-semiconductor interface properties. , 2013, , .		1
169	Biaxially strained extremely-thin body In0.53Ga0.47As-on-insulator metal-oxide-semiconductor field-effect transistors on Si substrate and physical understanding on their electron mobility. Journal of Applied Physics, 2013, 114, 164512.	1.1	16
170	InGaAsP Grating Couplers Fabricated Using Complementary-Metal–Oxide–Semiconductor-Compatible Ill–V-on-Insulator on Si. Applied Physics Express, 2013, 6, 042501.	1.1	28
171	Reduction in Interface Trap Density of Al <sub>2</sub> O <sub>3</sub> /SiGe Gate Stack by Electron Cyclotron Resonance Plasma Post-nitridation. Applied Physics Express, 2013, 6, 051302.	1.1	20
172	Atomic layer-by-layer oxidation of Ge (100) and (111) surfaces by plasma post oxidation of Al2O3/Ge structures. Applied Physics Letters, 2013, 102, .	1.5	22
173	High mobility strained-Ge pMOSFETs with 0.7-nm ultrathin EOT using plasma post oxidation HfO <inf>2</inf> /Al <inf>2</inf> 0 <inf>3</inf> /GeO <inf>x</inf> gate stacks and strain modulation. , 2013, , .		8
174	Impact of Fermi Level Pinning Due to Interface Traps Inside the Conduction Band on the Inversion-Layer Mobility in \$hbox{In}_{x}hbox{Ga}_{1 - x}hbox{As}\$ Metal–Oxide–Semiconductor Field Effect Transistors. IEEE Transactions on Device and Materials Reliability, 2013, 13, 456-462.	1.5	25
175	Formation of Ill–V-on-insulator structures on Si by direct wafer bonding. Semiconductor Science and Technology, 2013, 28, 094009.	1.0	47
176	Dark current reduction of Ge photodetector by GeO_2 surface passivation and gas-phase doping. Optics Express, 2012, 20, 8718.	1.7	138
177	Low-driving-current InGaAsP photonic-wire optical switches using III-V CMOS photonics platform. Optics Express, 2012, 20, B357.	1.7	34
178	Strained In0.53Ga0.47As metal-oxide-semiconductor field-effect transistors with epitaxial based biaxial strain. Applied Physics Letters, 2012, 100, 193510.	1.5	23
179	In0.53Ga0.47As metal-oxide-semiconductor field-effect transistors with self-aligned metal source/drain using Co-InGaAs alloys. Applied Physics Letters, 2012, 100, .	1.5	12
180	Numerical analysis of strained SiGe-based carrier-injection optical modulators. , 2012, , .		0

#	Article	IF	CITATIONS
181	High mobility CMOS technologies using III-V/Ge channels on Si platform. , 2012, , .		8
182	Self-aligned metal S/D GaSb p-MOSFETs using Ni-GaSb alloys. , 2012, , .		7
183	High mobility Ge pMOSFETs with 0.7 nm ultrathin EOT using HfO <inf>2</inf> /Al <inf>2</inf> O <inf>3</inf> /GeO <inf>x</inf> /Ge gate stacks fabricated by plasma post oxidation. , 2012, , .		17
184	Sub-60 nm deeply-scaled channel length extremely-thin body In <inf>x</inf> Ga <inf>1−x</inf> As-on-insulator MOSFETs on Si with Ni-InGaAs metal S/D and MOS interface buffer engineering. , 2012, , .		10
185	Improvement of SiGe MOS interfaces by plasma post-nitridation for SiGe high-k MOS optical modulators. , 2012, , .		1
186	1-nm-capacitance-equivalent-thickness HfO2/Al2O3/InGaAs metal-oxide-semiconductor structure with low interface trap density and low gate leakage current density. Applied Physics Letters, 2012, 100, .	1.5	146
187	Reduction in interface state density of Al2O3/InGaAs metal-oxide-semiconductor interfaces by InGaAs surface nitridation. Journal of Applied Physics, 2012, 112, 073702.	1.1	41
188	Initial Processes of Atomic Layer Deposition of Al2O3 on InGaAs: Interface Formation Mechanisms and Impact on Metal-Insulator-Semiconductor Device Performance. Materials, 2012, 5, 404-414.	1.3	18
189	Strain Engineering of Plasma Dispersion Effect for SiGe Optical Modulators. IEEE Journal of Quantum Electronics, 2012, 48, 8-16.	1.0	39
190	High-Mobility Ge pMOSFET With 1-nm EOT \$hbox{Al}_{2} hbox{O}_{3}/hbox{GeO}_{x}/hbox{Ge}\$ Gate Stack Fabricated by Plasma Post Oxidation. IEEE Transactions on Electron Devices, 2012, 59, 335-341.	1.6	168
191	Advanced CMOS technologies using III-V/Ge channels. , 2011, , .		0
192	Sub-10-nm Extremely Thin Body InGaAs-on-Insulator MOSFETs on Si Wafers With Ultrathin \$hbox{Al}_{2}hbox{O}_{3}\$ Buried Oxide Layers. IEEE Electron Device Letters, 2011, 32, 1218-1220.	2.2	60
193	Enhancement technologies and physical understanding of electron mobility in III–V n-MOSFETs with strain and MOS interface buffer engineering. , 2011, , .		24
194	Suppression of Interface State Generation in Si MOSFETs with Biaxial Tensile Strain. IEEE Electron Device Letters, 2011, 32, 1005-1007.	2.2	3
195	Highly-strained SGOI p-channel MOSFETs fabricated by applying Ge condensation technique to strained-SOI substrates. , 2011, , .		0
196	High mobility material channel CMOS technologies based on heterogeneous integration. , 2011, , .		2
197	Gas Phase Doping of Arsenic into (100), (110), and (111) Germanium Substrates Using a Metal–Organic Source. Japanese Journal of Applied Physics, 2011, 50, 010105.	0.8	11
198	Physical Origin of Drive Current Enhancement in Ultrathin Ge-on-Insulator n-Channel Metal–Oxide–Semiconductor Field-Effect Transistors under Full Ballistic Transport. Japanese Journal of Applied Physics, 2011, 50, 010110.	0.8	7

#	Article	IF	CITATIONS
199	Impact of Fermi level pinning inside conduction band on electron mobility of In <inf>x</inf> Ga <inf>1−x</inf> As MOSFETs and mobility enhancement by pinning modulation. , 2011, , .		23
200	Self-aligned metal source/drain InP n-metal-oxide-semiconductor field-effect transistors using Ni–InP metallic alloy. Applied Physics Letters, 2011, 98, 243501.	1.5	21
201	Highly strained-SiGe-on-insulator p-channel metal-oxide-semiconductor field-effective transistors fabricated by applying Ge condensation technique to strained-Si-on-insulator substrates. Applied Physics Letters, 2011, 99, .	1.5	25
202	Suppression of ALD-Induced Degradation of Ge MOS Interface Properties by Low Power Plasma Nitridation of GeO2. Journal of the Electrochemical Society, 2011, 158, G178.	1.3	30
203	III-V CMOS technologies on Si platform. Materials Research Society Symposia Proceedings, 2011, 1336, 50401.	0.1	0
204	Fabrication of Ge-rich SiGe-On-insulator waveguide for optical modulator. , 2011, , .		1
205	Al 2 O 3 / GeO x / Ge gate stacks with low interface trap density fabricated by electron cyclotron resonance plasma postoxidation. Applied Physics Letters, 2011, 98, .	1.5	143
206	Physical Origin of Drive Current Enhancement in Ultrathin Ge-on-Insulator n-Channel Metal–Oxide–Semiconductor Field-Effect Transistors under Full Ballistic Transport. Japanese Journal of Applied Physics, 2011, 50, 010110.	0.8	5
207	Ultrasmall Arrayed Waveguide Grating Multiplexer using InP-based Photonic Wire Waveguide on Si wafer for III-V CMOS photonics. , 2010, , .		9
208	A Novel Characterization Scheme of \$hbox{Si/SiO}_{2} Interface Roughness for Surface Roughness Scattering-Limited Mobilities of Electrons and Holes in Unstrained- and Strained-Si MOSFETs. IEEE Transactions on Electron Devices, 2010, 57, 2057-2066.	1.6	28
209	Impact of InGaAs surface nitridation on interface properties of InGaAs metal-oxide-semiconductor capacitors using electron cyclotron resonance plasma sputtering SiO2. Applied Physics Letters, 2010, 97, 132102.	1.5	29
210	Extremely-thin-body InGaAs-on-insulator MOSFETs on Si fabricated by direct wafer bonding. , 2010, , .		33
211	Advanced non-Si channel CMOS technologies on Si platform. , 2010, , .		2
212	III-V/Ge CMOS technologies on Si platform. , 2010, , .		13
213	High-Performance \$hbox{GeO}_{2}/hbox{Ge}\$ nMOSFETs With Source/Drain Junctions Formed by Gas-Phase Doping. IEEE Electron Device Letters, 2010, 31, 1092-1094.	2.2	86
214	High mobility III–V-on-insulator MOSFETs on Si with ALD-Al <inf>2</inf> O <inf>3</inf> BOX layers. , 2010, , .		3
215	Source/drain formation by using epitaxial regrowth of N+InP for III–V nMOSFETs. , 2009, , .		0
216	Evaluation of Electron and Hole Mobility at Identical Metal–Oxide–Semiconductor Interfaces by using Metal Source/Drain Ge-on-Insulator Metal–Oxide–Semiconductor Field-Effect Transistors. Japanese Journal of Applied Physics, 2009, 48, 04C050.	0.8	8

#	Article	IF	CITATIONS
217	InGaAsP Photonic Wire Based Ultrasmall Arrayed Waveguide Grating Multiplexer on Si Wafer. Applied Physics Express, 2009, 2, 122201.	1.1	38
218	High Electron Mobility Metal–Insulator–Semiconductor Field-Effect Transistors Fabricated on (111)-Oriented InGaAs Channels. Applied Physics Express, 2009, 2, 121101.	1.1	49
219	Comprehensive Understanding of Coulomb Scattering Mobility in Biaxially Strained-Si pMOSFETs. IEEE Transactions on Electron Devices, 2009, 56, 1152-1156.	1.6	13
220	On Surface Roughness Scattering-Limited Mobilities of Electrons and Holes in Biaxially Tensile-Strained Si MOSFETs. IEEE Electron Device Letters, 2009, 30, 987-989.	2.2	23
221	Design and fabrication of Mach-Zehnder interferometer bistable laser diode all-optical flip-flop. , 2009, , .		1
222	Metal source/drain inversion-mode InP MOSFETs. , 2009, , .		0
223	Surface orientation dependence of interface properties of GeO2/Ge metal-oxide-semiconductor structures fabricated by thermal oxidation. Journal of Applied Physics, 2009, 106, .	1.1	98
224	Experimental Study on Wavelength Tunability of All-Optical Flip-Flop Based on Multimode-Interference Bistable Laser Diode. IEEE Photonics Journal, 2009, 1, 40-47.	1.0	10
225	Carrier-Transport-Enhanced Channel CMOS for Improved Power Consumption and Performance. IEEE Transactions on Electron Devices, 2008, 55, 21-39.	1.6	324
226	Polarization-Insensitive All-Optical Flip-Flop Using Tensile-Strained Multiple Quantum Wells. IEEE Photonics Technology Letters, 2008, 20, 1851-1853.	1.3	7
227	InP–InGaAsP Integrated 1 \$imes\$ 5 Optical Switch Using Arrayed Phase Shifters. IEEE Photonics Technology Letters, 2008, 20, 1063-1065.	1.3	40
228	Evidence of low interface trap density in GeO2â^•Ge metal-oxide-semiconductor structures fabricated by thermal oxidation. Applied Physics Letters, 2008, 93, .	1.5	299
229	Ge photodetector integrated with Ge-on-insulator MOSFET by using oxidation condensation technique. , 2008, , .		1
230	Dynamic operation of polarization insensitive all-optical flip-flop based on multimode-interference bistable laser diode. , 2008, , .		0
231	Comprehensive understanding of surface roughness and Coulomb scattering mobility in biaxially-strained Si MOSFETs. , 2008, , .		10
232	Wavelength tunability of all-optical flip-flop using distributed Bragg reflectors. , 2008, , .		0
233	MMI bistable laser diode optical flip-flops for all-optical packet switching networks. Conference Proceedings - Lasers and Electro-Optics Society Annual Meeting-LEOS, 2007, , .	0.0	0
234	InP photonic wire waveguide using InAlAs oxide cladding layer. Optics Express, 2007, 15, 8422.	1.7	51

#	Article	IF	CITATIONS
235	Examination of Additive Mobility Enhancements for Uniaxial Stress Combined with Biaxially Strained Si, Biaxially Strained SiGe and Ge Channel MOSFETs. , 2007, , .		28
236	Characterization of interface properties of Al <sub>2</sub> O <sub>3</sub> /n-GaSb and Al <sub>2</sub> O <sub>3</sub> /InAs/n-GaSb metal-oxide-semiconductor structures. Japanese Journal of Applied Physics, 0, , .	0.8	0